ELSEVIER

Nuclear Physics A699 (2002) 65c–72c

NUCLEAR PHYSICS A

www.elsevier.com/locate/npe

A$(e, e'p)$ reactions at GeV energies

Dimitri Debruyne and Jan Ryckebusch * [a]

[a]Department of Subatomic and Radiation Physics, Ghent University, Proeftuinstraat 86, B-9000 Gent, Belgium

An unfactorized and relativistic framework for calculating A$(e, e'p)$ observables at typical JLAB energies is presented. Results of $(e, e'p)$ model calculations for the target nuclei ^{12}C and ^{16}O are presented and compared to data from SLAC and JLAB.

1. Introduction and physics motivation

Exclusive $A(e, e'p)$ reactions at sufficiently large values of the four-momentum transfer Q^2 are an excellent tool to learn more about different aspects of nuclear and nucleon structure in a regime where one expects that both hadronic and partonic degrees-of-freedom may play a role. Amongst the physics subjects which can be probed with the aid of exclusive electro-induced proton knockout from nuclei we mention the study of the short-range structure of nuclei. Here, one of the major questions to be addressed is whether there are any hadronic components in the nucleus that carry large momenta. Another question which has attracted the attention of the nuclear physics community for many years, is the apparent robustness of nucleons in the medium. Various techniques have been used to determine to what extent nucleons are modified in the medium. One of the more recent and more promising ones are double polarization $(\vec{e}, e'\vec{p})$ processes from nuclei [1]. These processes are meant to provide stringent tests of constituent-quark models predicting measurable medium modifications of the electromagnetic form factors of bound nucleons [2]. Another subject of current investigation is the problem of nuclear transparency in proton knockout from nuclei. Amongst other things, these investigations address the question whether there are any signatures for the onset of non-hadronic degrees of freedom for a given distance scale. The latter can be varied by exploring ranges of Q^2.

All of the above physics topics are awaiting further exploration at facilities like Jefferson Laboratory (JLAB), the Mainz microtron (MAMI) and the MIT-Bates electron accelerator, provided that one can develop reliable models which provide a realistic description of the final-state interactions (FSI) in A$(e, e'p)$ reactions. Popular frameworks to treat FSI effects in modelling $A(e, e'p)$ reactions can roughly be divided in two major classes. At "low" energies ($p_p \leq 1$ GeV/c) most models use optical potentials to determine the scattering wave function for the ejected proton. The parameters in the optical potentials are usually obtained from global fits to elastic $p + A$ scattering data and are available in both relativistic and non-relativistic forms. At higher energies ($p_p \geq 1$ GeV/c), on the other hand, the Glauber model offers good prospects to deal with the distortions which

*e-mail : jan.ryckebusch@rug.ac.be

PII S0375-9474(01)01471-3

the ejectile undergoes. In the Glauber model, the FSI is calculated directly from the elementary nucleon-nucleon scattering amplitudes $p + N \longrightarrow p + N$. One of the major goals of the work presented here, is to provide a framework in which the low and high-energy regime can be bridged. In particular, we deem that a "smooth transition" between the low and high-energy regime is a prerequisite for any model that claims to provide a realistic description of the final-state interactions (FSI). The separation between a "low" and "high-energy" regime in modelling FSI's, is usually done on the basis of the observation that for lab proton momenta p_p exceeding 1 GeV/c the elementary proton-nucleon scattering process becomes highly inelastic.

2. Relativistic Eikonal Model for A(e, e'p)

The model for the description of $A + e \longrightarrow (A-1) + e' + p$ processes which we developed has the following features. First, it can accommodate relativity in both the description of the electron-proton coupling and the nuclear dynamics. Further, it can be used in combination with both the "optical potential" and the "Glauber" framework for dealing with the final-state interactions. Furthermore, the framework does not use any partial-wave expansion in its numerical calculations and can therefore be used to calculate cross sections at very high values of Q^2 in a rather elegant manner. In our model, A$(\vec{e}, e'\vec{p})$ observables can be computed for any target nucleus with $A \geq 4$ provided that its ground-state wave function can be reasonably well described within the context of a relativistic mean-field model. Finally, we provide a completely unfactorized description of the reaction dynamics. This means that our model is **NOT** based on an expression of the type

$$\frac{d^6\sigma}{dT_p d\Omega_p d\epsilon' d\Omega_{\epsilon'}}(e, e'p) = \frac{p_p E_p}{(2\pi)^3}\sigma_{ep} P\left(\vec{p}_m, E_m\right) . \tag{1}$$

The use of this factorized expression was abandoned in the description of low-energy $A(e, e'p)$ process many years ago, but still seems to be common practice when it comes to modeling $A(e, e'p)$ processes at higher energies. In an unfactorized framework, the $A(\vec{e}, e'p)$ cross section takes on the well-known form in the one-photon exchange approximation

$$\frac{d^5\sigma}{d\Omega_p d\epsilon' d\Omega_{\epsilon'}}(\vec{e}, e'p) = \frac{1}{8\pi^3}\frac{M_p M_{A-1} p_p}{M_A} f_{rec}^{-1}\sigma_{Mott}$$
$$\times\left[v_T W_T + v_L W_L + v_{LT} W_{LT}\cos\phi_p + v_{TT} W_{TT}\cos 2\phi_p + h\left[v'_{LT} W'_{LT} + v'_{TT} W'_{TT}\right]\right] , \tag{2}$$

where h denotes the electron helicity and the structure functions W depend on the variables (q,ω,p_p,θ_p). In the Impulse Approximation (IA) the structure functions W are determined by matrix elements of the type

$$m_F^{fi}\left(J^\mu\right) = \langle K_f s_f \left| J^\mu \right| K_i s_i\rangle = \overline{u}_f \Gamma^\mu\left(K_f s_f, K_i s_i\right) u_i , \tag{3}$$

where in the final state one has a scattering wave function $u_f(K_f, s_f)$ and in the initial state a bound-state wave function $u_i(K_i, s_i)$. Further, $\Gamma^\mu(K_f\ s_f, K_i\ s_i)$ represents the off-shell electron-proton coupling. In our model the relativistic bound-state wave functions

are obtained within the context of the "$\sigma-\omega$ model" which is a relativistic quantum-field theory for nucleons (ψ) interacting through pions (π's), vector mesons (ρ's and ω's) and scalar mesons (σ's) [3]. The model is usually solved in the Hartree approximation by replacing the scalar and vector meson-field operators by their expectation values.

The determination of the off-shell electron-proton coupling is amongst the weakest parts of any relativistic approach to $A(e,e'p)$ processes ! Indeed, there is some arbitrariness which translates itself in a variety of recipes which all provide identical results for on-shell particles but may lead to substantially different predictions when off-shell nucleons are involved. Amongst the more popular forms for the electron-proton coupling which have been used over the years, we mention

$$\Gamma^{\mu}_{cc1} = G_M(Q^2)\gamma^{\mu} - \frac{\kappa}{2M}F_2(Q^2)(K_i^{\mu}+K_f^{\mu}) , \tag{4}$$

$$\Gamma^{\mu}_{cc2} = F_1(Q^2)\gamma^{\mu} + \imath\frac{\kappa}{2M}F_2(Q^2)\sigma^{\mu\nu}q_{\nu} . \tag{5}$$

In determining the scattering wave functions we adopt the relativistic eikonal approximation. This method belongs to the class of semi-classical approximations which become "exact" in the limit of small de Broglie (db) wavelengths, $\lambda_{db} \ll a$, where a is the typical range of the potential in which the particle is moving. For a particle moving in a relativistic (optical) potential, the scattering wave function has the following form in the eikonal approximation

$$\psi^{(+)}_{\vec{k},s} \sim \left[\begin{array}{c} 1 \\ \frac{1}{E+M+V_s-V_v}\vec{\sigma}\cdot\vec{p} \end{array} \right] e^{\imath\vec{p}_p\cdot\vec{r}} e^{\imath S(\vec{r})} \chi_{\frac{1}{2}m_s} . \tag{6}$$

This wave function differs from a relativistic plane wave in two respects. First, there is a dynamical relativistic effect from the scalar V_s and vector V_v potential, which enhances the contribution from the lower components. Second, the wave function contains an eikonal phase which is determined by integrating the central (V_c) and spin-orbit (V_{so}) parts of the distorting potentials along the escaping particle's (asymptotic) trajectory ($\vec{r} \equiv (\vec{b},z)$)

$$\imath S(\vec{b},z) = -\imath\frac{M}{K}\int_{-\infty}^{z} dz' \left[V_c(\vec{b},z') + V_{so}(\vec{b},z')[\vec{\sigma}\cdot(\vec{b}\times\vec{K}) - \imath K z'] \right] , \tag{7}$$

where $\vec{K} \equiv \frac{1}{2}(\vec{p}_p+\vec{q})$. For proton lab momenta exceeding 1 GeV/c, the use of optical potentials is no longer justifiable in view of the highly inelastic character of the elementary processes. In this energy regime, an alternative description of FSI processes is provided in terms of the Glauber multiple-scattering theory. In such a framework the A-body wave function in the final state reads

$$\psi^{(+)}_{\vec{k},s} \sim \hat{\mathcal{S}} \left[\begin{array}{c} 1 \\ \frac{1}{E+M}\vec{\sigma}\cdot\vec{p} \end{array} \right] e^{\imath\vec{p}_p\cdot\vec{r}} \chi_{\frac{1}{2}m_s} \Psi^{J_R\,M_R}_{A-1}(\vec{r}_2,\vec{r}_3,\ldots\vec{r}_A) . \tag{8}$$

In this expression, the subsequent elastic or "mildly inelastic" collisions with "frozen" spectator nucleons which the ejectile undergoes, are implemented through the introduction of the following operator

$$\hat{\mathcal{S}}(\vec{r},\vec{r}_2,\vec{r}_3,\ldots\vec{r}_A) \equiv \prod_{j=2}^{A}\left[1-\Gamma\left(\mid\vec{p}_p\mid,\vec{b}-\vec{b_j}\right)\theta(z-z_j)\right] ,$$

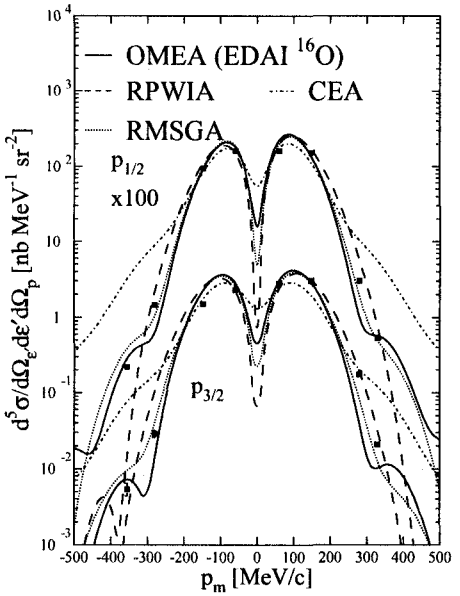

Figure 1. CEA, OMEA, RMSGA and RPWIA calculations (see text for details) for ^{16}O$(e, e'p)$ differential cross sections in quasi-perpendicular kinematics at ϵ = 2.4 GeV, q = 1 GeV/c and ω = 0.439 GeV. The calculations use the CC1 off-shell electron-proton coupling. The data are from Ref. [6].

where the profile function for elastic pN scattering reads

$$\Gamma(p_p, \vec{b}) = \frac{\sigma_{pN}^{tot}(1 - i\epsilon_{pN})}{4\pi\beta_{pN}^2} exp\left(-\frac{b^2}{2\beta_{pN}^2}\right) .$$

In practice, for a given ejectile's lab momentum the following input is required : the total proton-proton and proton-neutron cross sections σ_{pN}^{tot}, the slope parameters β_{pN} and the ratios of the real to imaginary scattering amplitude ϵ_{pN}.

3. Results

3.1. ^{16}O(e, e'p) : ω = 0.439 GeV and Q^2 = 0.8 (GeV/c)^2

We have compared our relativistic calculations to recent quasi-elastic ^{16}O$(e, e'p)$ data from JLAB. In these high-resolution experiments at Q^2 = 0.8 (GeV/c)^2 separated structure functions and polarization transfer data were obtained. In the considered kinematics the de Broglie wavelength of the ejected proton is of the order $\lambda_{db} \approx 0.2$ fm and one may expect the eikonal and Glauber framework to be applicable. At the same time, at these kinetic energies, optical potentials are still readily available. In Figure 1 we display the calculated differential cross sections against the missing momentum.

The different curves all use the same bound-state wave functions and electron-proton coupling but differ in the way the FSI is treated. The adopted techniques are

1. A Relativistic Plane Wave Impulse Approximation (RPWIA) calculation in which the ejectile is described by a relativistic plane wave.
2. A so-called Consistent Eikonal Approximation (CEA) calculation [4]. Here, the eikonal phase (7) is calculated from the relativistic scalar and vector potentials which determine also the bound-state wave functions.
3. An Optical-Model Eikonal Approximation (OMEA) calculation. Here, the eikonal phase (7) is calculated from the relativistic optical potentials as they are derived from global fits to elastic proton-nucleus data. We use the energy-dependent mass number independent (EDAI) version of Ref. [5].
4. A Relativistic Multiple-Scattering Glauber Approximation (RMSGA) calculation. In this approach, the scattering state is calculated on the basis of Eq. (8).

The CEA approach, despite the fact that it obeys orthogonality and unitarity constraints, fails to predict the missing-momentum dependence of the measured cross sections. The RMSGA and the OMEA approach, on the other hand, both seem to give a reasonable description of the data. A similar remark holds for the separated structure functions (not shown here) and the polarization transfer data. Several relativistic calculations based on optical potentials nicely agreed with the ^{16}O$(e,e'p)$ data set [6]. The novel thing about the results displayed in Figure 1, is that also an out-of-the box relativistic calculation within the Glauber framework produces fair results. To illustrate this further, we display in Fig. 2 the left-right asymmetry

$$A_{LT} = \frac{\sigma(\phi = 0°) - \sigma(\phi = 180°)}{\sigma(\phi = 0°) + \sigma(\phi = 180°)} = \frac{v_{LT} W_{LT}}{v_L W_L + v_T W_T + v_{TT} W_{TT}} \,. \tag{9}$$

This quantity is highly sensitive to relativistic effects [6,10]. At higher missing momenta, the A_{LT} data strongly deviate from the RPWIA predictions pointing towards important FSI effects. Both the Glauber-based RMSGA and the optical-potential based OMEA approach provide a reasonable description of the high-p_m data points.

Spectroscopic factors are extracted quantities which normalize a theory to the data. Recent investigations [7,8] point towards the rather intriguing situation that the spectroscopic factors extracted at higher values of Q^2 turn out to be substantially larger than those derived at lower values of Q^2 [9]. This phenomenon, which has been dubbed as "quenching disappearance" may point towards a scale dependence in nuclear physics. It turns out, however, that all the "higher" values for the spectroscopic factors are obtained within the Glauber approach whereas the lower values are extracted by comparing optical-model calculations with data. One could wonder whether there is any real physics behind this. It may as well be that these observations regarding the value of spectroscopic factors reflect the inability of the theorists to treat the FSI in $(e,e'p)$ processes and to provide model calculations that ensure a smooth transition between the "low-energy" (optical-potential) and the "high-energy" (Glauber inspired) regime. Our framework has the feature of being able to deal with optical potentials as well as the Glauber approach, as long as one works in kinematic regimes where the eikonal approximation appears plausible. We asked ourselves the question whether the Glauber and optical potential approach produce the same spectroscopic factors for the kinematics of the ^{16}O results in Figs. 1

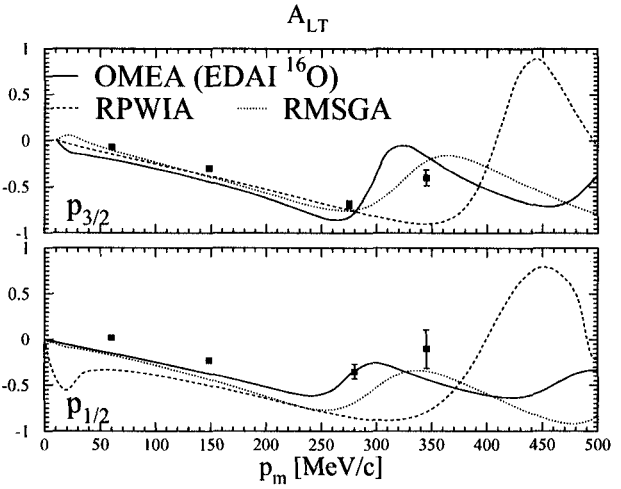

Figure 2. Left-right asymmetry for the quasi-elastic ^{16}O$(e,e'p)$ cross sections of Fig. 1.

	OMEA (CC1)	RMSGA (CC1)	OMEA (CC2)	RMSGA (CC2)
$\frac{1}{2}^-$ (g.s)	0.79 (0.60)	0.80 (0.38)	0.82 (1.04)	0.82 (0.95)
$\frac{3}{2}^-$ (6.31 MeV)	0.96 (1.78)	0.96 (0.75)	1.00 (3.48)	1.00 (2.19)

Table 1
The spectroscopic factors (normalized to 1) for the ^{16}O$(e,e'p)$ reaction in the kinematics of Fig. 1. The obtained χ^2 per degree-of-freedom is given between brackets.

and 2. Therefore, a fit of the calculations to the data was performed, including the results for the differential cross sections and the separated structure functions. The results are summarized in Table 1. We find that the Glauber and optical potential framework lead to almost identical spectroscopic factors, which are significantly larger than what was typically found at lower values of Q^2.

3.2. Nuclear transparency in ^{12}C

The nuclear transparency provides a measure of the likelihood that a struck "nucleon" escapes from the system. The Q^2 and A dependence of this quantity can provide information about point-like configurations (PLC) in the nucleus and the onset of non-hadronic degrees of freedom. Experimentally, the transparency is determined by taking the ratio of the integrated measured A$(e,e'p)$ strength over certain energy ΔE and momentum $\Delta^3 k$ ranges to the non-relativistic (NR) PWIA prediction. Typical ranges for light nuclei are determined by the Fermi momentum $p_m \leq k_F$ and the excitation-energy where all the single-particle strength is expected to reside, i.e. $E_m \leq 60$ MeV. We have computed the

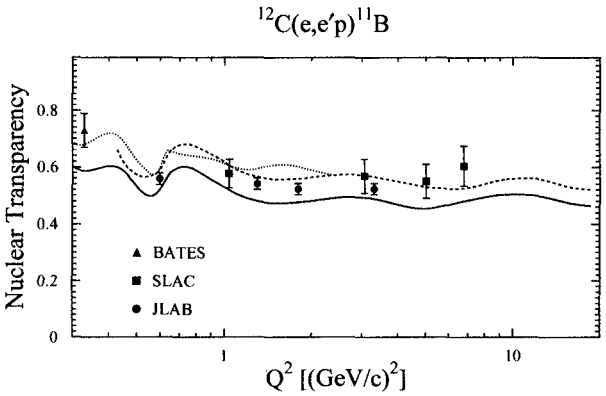

Figure 3. Nuclear transparency for ^{12}C$(e, e'p)$ as a function of Q^2. The theoretical predictions are obtained within the RMSGA (solid line) and OMEA (dotted line). The dashed line is the RMSGA result after including SRC effects. The calculations use the CC2 form for the electron-proton coupling.

nuclear transparency according to

$$T_{th} = \frac{\sum_\alpha \int_0^{k_F} d\vec{k} \frac{\frac{d^5\sigma}{d\Omega_p dc' d\Omega_{c'}}(e,e'p_\alpha)}{K\sigma_{ep}^{CC1}}}{\sum_\alpha \int_0^{k_F} d\vec{k}\, S^\alpha_{NRPWIA}(\vec{k})}, \tag{10}$$

where the sum over α extends over all occupied single-particle states of the target nucleus.

The description of the nuclear transparency at higher Q^2 requires the inclusion of effects from short-range correlations (SRC). The inclusion of SRC causes an overall enhancement of the nuclear transparency with some 10 %. No Q^2 dependent increase of the nuclear transparency with increasing momentum transfers is observed. As was pointed out in Refs. [7] and [8], the ^{12}C nuclear transparencies can be linked to the summed spectroscopic factor of the 1s and 1p levels. The $Q^2 > 1$ (GeV/c)^2 results in Fig. 3 are compatible with a summed spectroscopic factor which is Q^2 independent and substantially larger than what is commonly found at low values of Q^2. Another important finding from Fig. 3 is that when it comes to describing FSI effects in A$(e, e'p)$ transparency calculations, the optical-potential and Glauber framework provide reasonably consistent results, provided that the Glauber calculations are corrected for SRC effects. Indeed, in the regime where both the optical-potential and the Glauber approach appear justified, both predict comparable transparency results, including the structures in the Q^2 dependence of the transparency at lower values of Q^2.

4. Conclusion

Summarizing, a flexible framework for modeling A$(e, e'p)$ processes at high values of the four-momentum transfer has been presented. The model is relativistic and fully unfactor-

ized and can be used in combination with optical potentials, when available, as well with the Glauber multiple-scattering approach for the treatment of the final-state interactions. One of the major conclusions of our investigations is that the Glauber framework, in which the final-state interactions are computed directly from the elementary proton-nucleon processes, works reasonably well even when it comes to predicting polarization observables and separated structure functions. The relativistic effects on the total cross sections are relatively small. Some structure functions, for example the longitudinal-transverse interference term R_{LT}, turn out to be highly sensitive to relativistic effects, an observation which was earlier made in d$(e, e'p)$ studies.

Our unfactorized and relativistic Glauber framework provides a reasonable description of the measured ^{12}C$(e, e'p)$ nuclear transparencies. In these transparency calculations, we observe a relatively "smooth" transition between the energy regime where optical potentials can be used and the high-energy regime where the use of the Glauber framework appears legitimate. In the energy regime where both the "optical potential" and the "Glauber" treatment of final-state interactions appear justified, both approaches give similar results provided that the free proton-nucleon cross sections are corrected for short-range correlations in the target nucleus. From our calculations we have two arguments which seem to support the "quenching disappearance" phenomenon at higher values of Q^2. The spectroscopic factors which are extracted from comparing our relativistic eikonal calculations to the extensive ^{16}O$(e, e'p)$ data set at $Q^2 = 0.8$ (GeV/c)^2, which includes separated structure functions and differential cross sections, are substantially higher than the values obtained at lower values of Q^2. One striking feature is that the Glauber and "optical potential" treatment of final-state interactions, which are intrinsically very different, lead to almost identical values for the extracted spectroscopic factors. Also a comparison of the relativistic eikonal predictions with the available ^{12}C$(e, e'p)$ transparency data, is consistent with values of the summed spectroscopic strength which almost exhaust the sum-rule value when integrated over the first 60 MeV in missing energy of ^{11}B.

REFERENCES

1. S. Dieterich *et al.*, Phys. Lett. **B500** (2001) 47.
2. R. Ransome, contribution to this conference.
3. B. Serot and J. Walecka, Adv. Nucl. Phys. **16** (1986) 1.
4. Dimitri Debruyne, Jan Ryckebusch, Wim Van Nespen and Stijn Janssen, Phys. Rev. C **62** (2000) 024611.
5. E. Cooper, S. Hama, B. Clarck and R. Mercer, Phys. Rev. **C47** (1993) 297.
6. J. Gao *et al.*, Phys. Rev. Lett. **84** (2000) 3265.
7. L. Lapikás, G. van der Steenhoven, L. Frankfurt, M. Strikman and M. Zhalov, Phys. Rev. C **61** (2000) 064325.
8. L. Frankfurt, M. Strikman and M. Zhalov, Phys. Lett. **B503** (2001) 73.
9. V. Pandharipande, I. Sick and P. deWitt Huberts, Rev. Mod. Phys. **69** (1997) 981.
10. J. Ryckebusch, D. Debruyne, W. Van Nespen and S. Janssen, Phys. Rev. **C60** (1999) 034604.